SLOWING DOWN OF MULTICHARGED IONS IN SOLIDS AND GASES

Ya. A. TEPLOVA, V. S. NIKOLAEV, I. S. DMITRIEV, and L. N. FATEEVA

Institute of Nuclear Physics, Moscow State University

Submitted to JETP editor July 12, 1961

J. Exptl. Theoret. Phys. (U.S.S.R.) **42**, 44-60 (January, 1962)

The ranges and specific energy losses of fast He, Li, Be, B, C, N, O, Ne, Na, Mg, Al, P, Cl, K, Br, and Kr ions having velocities between 2.6×10^8 and 11.8×10^8 cm/sec are measured in hydrogen, helium, methane, benzene, air, argon, and various mixtures of these gases. The specific energy losses in celluloid, Al, Ni, Ag, and Au are also measured. The dependences of the ion range and specific energy loss on the ionic nuclear charge Z are not monotonic; this is accounted for by the electronic structures of the different atoms. The effective ion charge is 10—20% larger than the mean charge in the equilibrium distribution. The decrease of stopping power as Z increases is much more pronounced for the solids than for the gases. However, the mean energy losses in gases and solids do not differ greatly. It is shown that the energy loss due to charge exchange does not exceed 25% of the total energy loss.

SEVERAL groups of investigators have recently measured the ranges of multicharged ions having energies from 1 to 10 MeV per nucleon,[1-3] and the specific energy losses of C, O, and N ions having 0.02 to 0.25 MeV/nucleon in solids.[4,5] However, our experimental information concerning the stopping of multicharged ions is still fragmentary. This situation hinders the derivation of an approximate analytical dependence of ion range R and of specific energy loss dE/dx on the ionic atomic number Z, the atomic number Z_S of the stopping material, and the ion velocity v at energies below 1—2 MeV/nucleon.

The present work consists of measurements of R, dE/dx, and the range straggling S of multicharged ions having energies from 25 to ~700 keV/nucleon, over broad ranges of Z and Z_S in solids and gases. Preliminary results have been published in [6].

APPARATUS AND EXPERIMENTAL TECHNIQUE

As in our earlier work,[7] we used beams of multicharged ions extracted from a 72-cm cyclotron. Particle velocities were determined from the field of the focusing magnet, which had been calibrated to within ~ 2%, over the entire interval of magnetic field variation, from the ranges of protons and α particles with eight different energies. Sufficiently good focusing was obtained over the entire working range of focusing field strength. The energy spread of the ion beam did not exceed ±1%. In addition to a considerable increase in the amount of data compared with [7], the accuracy of the measurements was enhanced by several improvements.

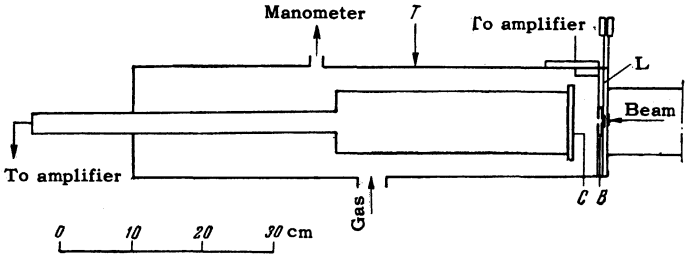

FIG. 1. Schematic diagram of measuring apparatus. T — stopping chamber, L — vacuum lock, C — multiwire counter, B — monitor counter.

Figure 1 shows the general scheme of the apparatus. The ion beam entered the stopping chamber T through celluloid films 30—50 $\mu g/cm^2$ thick (approximately $\frac{1}{3}$ to $\frac{1}{4}$ the thickness used in [7]). Films were changed without disturbing the vacuum by means of a special vacuum lock L. The principal parts of this lock were two plates moving parallel to each other in the vacuum, each plate having three apertures. One aperture in each plate was open, while the others were covered with films. Different combinations of apertures provided for the measurement of film thickness from the range difference with and without film. The same lock was used to measure the air equivalents of unsupported metallic films.

Ions were registered by a multiwire flat proportional counter C in the form of a cylinder 6

mm high and 80 mm in diameter. Charged particles entered the counter through slits 3 mm wide in the cylinder base, which served as the high-potential electrode. The collecting electrode consisted of tungsten wires, 60 μ in diameter, stretched in the middle of the space between the cylinder ends. The wires were parallel to the slits with sufficient displacement to prevent direct impingement of the ion beam. The selected counter diameter was based on an analysis of the angle spread φ in a beam of N ions. φ was measured by a counter with a narrow 3 × 10 mm slit equal to the entrance slit of the chamber T. The counter slit was positioned alternately parallel and perpendicular to the entrance slit. At 40 mm Hg air pressure in T for N ions with $v = 7.9 \times 10^8$ cm/sec, we measured $\varphi = 5°$. Under the actual experimental conditions the smallest angle subtended by the multiwire counter (with 80 mm diameter) was 18°. Therefore the measurements of R and dE/dx were not affected by an error associated with scattering of the particles.

The chamber T and the counters were filled [7] with chemically pure H_2, He, CH_4, C_2H_4, Ar, and various mixtures of these gases, and with air or benzene vapor C_6H_6. Gas pressures were measured with an inclined mercury manometer calibrated to within ± 0.1 mm Hg by a U-shaped oil manometer. In the work with hydrogen the gas pressure was usually ~ 230 mm and the counter potential was ~ 1200 V. For air we used 42 ± 2 mm pressure and ~ 700 V; for C_6H_6 we used ~ 10 mm pressure and 700 V etc. The addition of a small (~ 1%) admixture of CH_4, C_2H_4, or C_6H_6 in Ar, or ~ 1% Ar in He, increased ionization pulse amplitudes compared with the pure gases. The greatest increase, by a factor of several times unity, resulted from the addition of C_6H_6. In all instances the ionization potential of the admixture was lower than that of the main gas. Enhanced ionization resulted from an increased amount of ion pairs due to the ionization of impurity molecules by the transfer of excitation from molecules of the main gas, as well as from an increased gas amplification coefficient resulting from the depressed average ionization potential of the mixture. The increase of pulse height was identical over the entire range; therefore the registration of excited atoms did not affect the final results.

The technique used in measuring R and dE/dx has been described in detail in [6] and [7]. The mean and extrapolated ranges, R and R′, were determined within 2—3% from the curve for the relative number of counter pulses versus the distance between the counter and the entrance window of the chamber T. The maximum ranges R″ [6] and the specific energy losses dE/dx in the gases were measured from the counter pulse amplitudes. [6,7] R″ was measured within ± 3—7%, while dE/dx was measured within ± 5—15%. The substitution of R″ for R did not affect dE/dx within experimental error limits.

Because of the short ranges and low ion beam intensities only the maximum ranges were measured in the cases of Be, C, Na, Mg, Cl, K, Br, and Kr ions. A comparison of the mean and extrapolated ranges with the maximum ranges therefore constituted an important methodological problem; the results are given in Table I. R″ is seen to exceed R′ by 3—5%, while $S/R = (R' - R)/R$ reaches 2—9% (with $R'' - R' \leq R' - R$).

The values obtained for $R'' - R = \Delta R$ and S necessarily include the energy spread of the ion beam, as well as statistical and other errors. However, as we have shown in [7], the range straggling due to a nonmonoenergetic beam was in all instances considerably smaller (< 1%) than the measured values of S and ΔR. This conclusion is supported (within experimental error limits) by the agreement between our values of S for

Table I

Ion	Stopping gas	10^{-8} v, cm/sec	R, mm (760 mm Hg, 19°C)	$\frac{S}{R}$, %	$\frac{R'' - R'}{R}$, %
He	Air	5.3	3.4±0.1	3.5	3.1
		16.9	45.1±0.2	2.0	0.5
		19.4	70.4±1.2	1.5	1.3
Li	Argon	8.3	8.2±0.2	4.3	5.5
		11.7	16.5±0.3	2.8	4.0
B	Argon	8.1	7.5±0.2	3.5	2.5
		11.5	14.2±0.3	3.0	0.5
N	Argon	8.1	6.8±0.2	3.8	1.8
Ne	Air	4.1	3.3±0.2	7.0	2.8
		5.6	4.8±0.2	7.5	4.5
Al	,,	4.2	4.4±0.2	10.0	3.0
P	,,	4.1	4.2±0.2	9.0	4.5
Ar	,,	4.15	4.8±0.2	7.0	1.2

He ions in air at $v = 16.9 \times 10^8$ and 19.4×10^8 cm/sec and the published results for α particles from Po and ThC'.[8] The velocity spread for multicharged ions should not be greater than for α particles, since the focusing properties of the cyclotron extracting system are independent of the kind of ion.

Specific energy losses in solids were calculated from data on the air equivalents of films for different velocities and from the dependence of R on v in air. The measured result, $\Delta E/\Delta x$ with $\Delta E = E - E_1$, was taken as dE/dx, pertaining to the energy $(E + E_1)/2$, where E and E_1 are the ion energy before and after passing through the film, respectively. In addition to celluloid we used films of Al, Ni, Ag, and Au, varying in thickness from 50 to 350 $\mu g/cm^2$, prepared by vacuum evaporation on a celluloid backing that was subsequently dissolved. For each material dE/dx was measured with films of different thicknesses that varied by a factor of 2 to 3. The maximum error of the relative air equivalents of the films was ±7—10%, and the absolute error of the specific energy losses was ±10—15%. Control measurements with He ions showed that the values of dE/dx in celluloid, Al, and Ag agree within experimental error limits with data published in Whaling's review[9] and in [4], where celluloid was compared with Be since the corresponding values of Z_S are close.

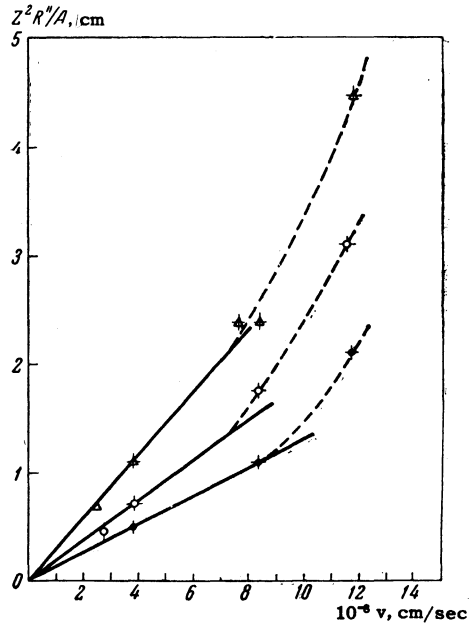

FIG. 2. Velocity dependence of R″ in methane at 760 mm Hg and 19°C for Li (●), B (○), and N (△) ions. (For units independent of the ion mass number A, values of $R''Z^2/A$ are given.) Continuous lines represent the linear portion of the R″ – v relation.

The values of dE/dx for α particles in Au and Ni films were 20—30% above the tabulated values in [9]. This discrepancy and an analysis of film composition revealed the presence of a residual celluloid layer. The thickness of the celluloid was determined from measurements with α particles, using the additive law of stopping powers, and was taken into account in measurements on multicharged ions in these films.

RANGES OF MULTICHARGED IONS

1. Experimental results. We measured the ranges of ions from He to Kr having velocities $(2.6—11.8) \times 10^8$ cm/sec in different gases (Figs. 2 and 3). The ranges obtained for He, Li, B, N, and Ne ions in air, argon, and hydrogen agreed with [7] within experimental error limits. In view

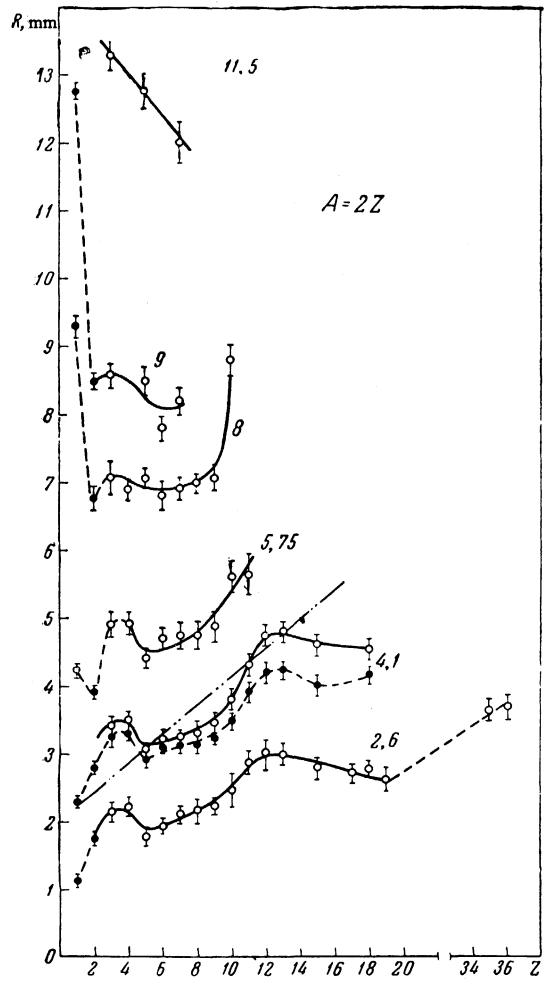

FIG. 3. Dependence of multicharged-ion ranges on Z in air at 760 mm Hg and 19°C. R″ – open circles connected by continuous lines; R – filled circles connected by dashed lines. The curves are labeled with the respective ion velocities in units of 10^8 cm/sec. The dot-dash straight line was computed from Eq. (1) for $v = 4.1 \times 10^8$ cm/sec.

of the fact that mean ranges were not measured for all ions and that R and R″ are represented by almost identical curves (Fig. 3), in the present paper as in [7] we give the values of R″. In the case of a nonmonoenergetic beam only R′ is usually measured. The experimental results showed that the ratios R/R′ and R/R″ for multicharged ions, particularly for Li, B, and N in methane, air, and argon, are independent of Z_S for a given velocity; this also holds true for α particles.[9] R can be obtained from these relations when R′ is known for a given medium, if both quantities are known for some other medium.

The velocity dependence of ion ranges is illustrated in Fig. 2. For ions with $Z \geq 2$ at low velocities R = kv is accurate to within 5—7%. The maximum velocity v_m at which this equation still holds true (with a discrepancy not greater than +5%) fluctuates in the interval $(5-8) \times 10^8$ cm/sec for ions from He to Ne. For protons $v_m \approx 1.2 \times 10^8$ cm/sec. At high velocities $R = kv^{\alpha}$, where $\alpha > 1$.

With increasing Z the proportionality coefficient k increases as $\sim Z^{1/2}$ on the average. For example, in air $k \sim 0.7$ for B ions and $k \approx 1.2 \pm 0.1$ for Ar ions (with R″ given in mm and v in units of 10^8 cm/sec). However, unlike the high-velocity region, where $R = MZ^{-2}f(v) + \Delta$,[8] in the investigated range of v and v = const the dependence of R″ on Z is nonmonotonic, and is characterized by periodic increases and decreases of the order of 30% (Fig. 3). The first peak of the R(Z) curve is located at Z = 3—4, and the second peak at Z = 11—13. The amplitude of the fluctuations diminishes with increasing velocity. A smoother curve is found for the dependence of R″ on $\overline{i^2}$, the mean square charge at a given velocity.[10]

In order to determine the relative stopping powers of different gases we measured the ranges of He, Li, B, N, and Ne ions in hydrogen, helium, argon, CH_4, C_2H_4, C_6H_6 vapor and various gaseous mixtures. The ratio of each of these ranges to the corresponding range in air was only slightly dependent on velocity. As the velocity increased until multiplied by the factor 2 the ratio fluctuated within the limits ±5%, and varied less than ±10% from ion to ion. The ranges of He, Li, B, and N ions in hydrogen are ~3.8 times greater, and in helium ~5.3 times greater, than in air, while in benzene vapor at 760 mm they are smaller by a factor ~3.5 than in air. (The results for He agreed with those published in [9].) For He and Li ions the ranges in methane are ~15% greater than in air, while for B and N ions they differ from the ranges in air by less than 5%. The ranges of N ions were measured in the largest number of stopping media. The dependence of R on Z_S was found to be similar to that for protons.[9] In all the investigated media at $v \approx 8 \times 10^8$ cm/sec we have $R_N/R_p = 1.6 \pm 0.1$ (Table II).

Table II

Stopping gas	$10^3 R''_N$, g/cm²	$10^3 R_p$ g/cm²[9]	R''_N/R_p
H_2	0.22	0.14	1.57
He	0.64	0.40	1.60
C_2H_4	0.60	—	—
CH_4	0.54	0.32	1.68
C_6H_6	0.05	—	—
Air	0.88	0.58	1.52
Ar	1.30	0.86	1.51

A corresponding similarity is also characteristic of other multicharged ions at $v \sim 10^8$—10^9 cm/sec, as well as for α particles[9] and fission fragments.[11]

The absolute value of the range straggling S diminishes somewhat with decreasing velocity, but the ratio $\delta = S/R$ increases. For α particles when the velocity is reduced to about ⅓ (from $\sim 2 \times 10^9$ to $\sim 6 \times 10^8$ cm/sec) δ increases by the factor 2.5. At constant velocity S and δ depend on Z nonmonotonically. The peaks of the curve representing the dependence of δ on Z are located in the same ranges of Z as on the curve for R. The largest value of δ is found for Al and P (~9%), and the smallest value is found for N (~3%) at $v \sim 4 \times 10^8$ cm/sec. The measured values of δ for α particles at $v = 5.8 \times 10^8$ cm/sec are close to those given in [9] and [12] for protons of the same velocity.

We did not obtain sufficient data to establish the dependence of δ on Z_S. However, we can state that δ is smaller in Ar than in air by a factor ~1.5.

2. Discussion of results. A simple range-velocity dependence R = kv of charged particles follows from the Fermi-Teller[13] and Firsov[14] formulas. Both formulas are rigorously applicable when $v \leq v_0$, where $v_0 = 2.19 \times 10^8$ cm/sec, the first formula for the stopping of singly-charged particles and the second for multicharged ions with $Z \sim (\frac{1}{4}-4)Z_S$. A similar relation $R = kv - \Delta_1$ has been observed for recoil nuclei with M ~ 150—120 in air and Al at $v = (5-15) \times 10^8$ cm/sec.[15] Here the coefficient k agrees within 15—20% with that given above. Thus R = kv represents the behavior of different ions at low velocities.

The fluctuations of R and S as Z is varied in-

dicate a significant role for the electronic structure of the ions. Similar fluctuations at v = const are observed in the dependence of the degree of ionization $\bar{i}/Z$ on Z. The regions of the maxima coincide approximately. The first maximum represents ions where the L shell begins to be filled, with the second maximum, correspondingly, for the M shell. With increasing ion velocity the fluctuations diminish; the details of the electronic structure become less important.

It was shown in [1] that the ranges of ions from C to Ar having energies 2—10 MeV/nucleon in nuclear emulsion can be represented by

$$R_Z = MZ^{-2}R_p + MZ^{2/3}C(v/v_k), \quad (1)$$

where M is the ion mass in atomic units, R_p is the range of a proton having velocity v, $v_k = v_0 Z$ is the velocity of K electrons, and the function $C(v/v_k)$ is identical for all ions. In our energy region the ranges of all ions with $Z > 4$ in methane, air, and argon can be represented by this equation to within ±10—15%, and for $v/v_k \leq 1$ we have $C(v/v_k) = 0.23\, v/v_k$ mm. The ranges of Li and Be ions differ from the general formula by ~ 20—30%, while for α particles the discrepancy is 30—50%.

When α-particle ranges are used instead of proton ranges the discrepancy of the general formula is reduced to 10—15% for light multicharged ions (Li, Be). When the velocity v_k is replaced by the electron velocity $v' = v_0 Z^{2/3}$ from the Thomas-Fermi model, this discrepancy is not reduced. The ranges of different ions, calculated from Eq. (1) are shown in Fig. 3. The formula obviously gives only the average dependence of R on Z, and does not indicate the individual peculiarities of ion ranges.

Computations of the statistical range straggling from the formulas of Bethe,[8] Bohr,[16] Lindhard et al,[17] and Sternheimer[18] give a value of S/R that agrees satisfactorily with experiment. However, none of these formulas reflects the nonmonotonic dependence of δ on Z at low velocities. The large increase of δ for $Z \geq 11$—15 can be accounted for by an additional spread due to elastic nuclear collisions of ions with atoms of the stopping material. It is difficult to determine the absolute magnitude of this "nuclear" straggling, since the relative number of nuclear collisions involved in the stopping of ions is not known precisely. However, it follows from experimental data on recoil data[15] that this fraction is appreciable and in some cases amounts to ~ 25%.

SPECIFIC ENERGY LOSSES

1. Experimental results. The specific energy losses dE/dx of ions from He to Ne were measured at velocities from 10^8 to 10^9 cm/sec in hydrogen, helium, methane, benzene, air, and argon (Figs. 4 and 5). The results for dE/dx in gaseous mixtures (Ar + He, Ar + CH_4, and Ar + C_6H_6) of varying relative concentrations showed that the additive law for multicharged ions is satisfied exactly as in the cases of protons and α particles.[9]

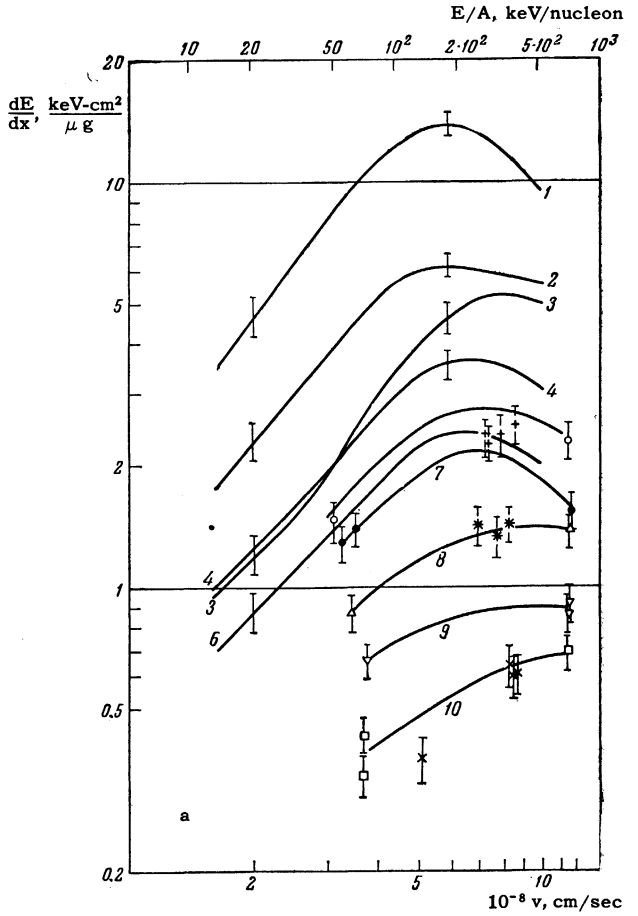

FIG. 4a. Velocity dependence of dE/dx for Li ions [and similarly for B ions (Fig. 4b), N ions (Fig. 4c), and Ne ions (Fig. 4d)]. The curves for dE/dx in the gases are averaged, with continuous lines representing our results and dashed lines representing data from[9]. Vertical bars indicate the maximum possible errors. 1 – in hydrogen; 2 – in methane; 3 – in helium; 4 – in air; 5 – in benzene; 6 – in argon. Our values for dE/dx in solids are denoted by the following symbols: ○ – in celluloid, ● – Al, △ – Ni, ▽ – Ag, □ – Au; these are connected by continuous lines. The data of other authors are represented as follows: . . . . . [4] (curve 7 in Al, 8 in Ni, 9 in Ag, 10 in Au); – – . – – [19] and + [9] in Al; . – . – [2] * [9] in Ni; × [9] in Au; – . . – . . [1] in emulsion. The continuous curve labeled Bl was computed from Bloch's formula for B in hydrogen; the straight lines –‖–‖–‖– were computed from Firsov's formula.

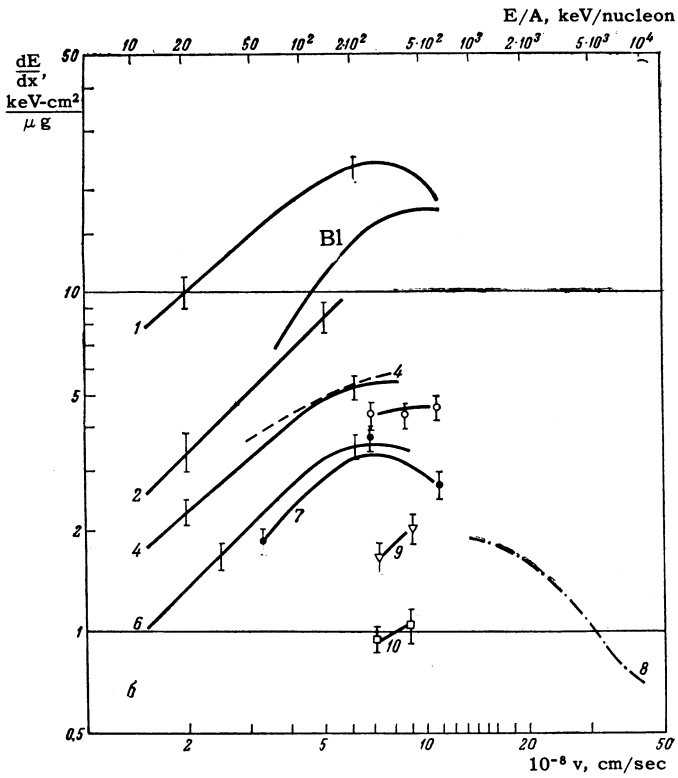

FIG. 4b

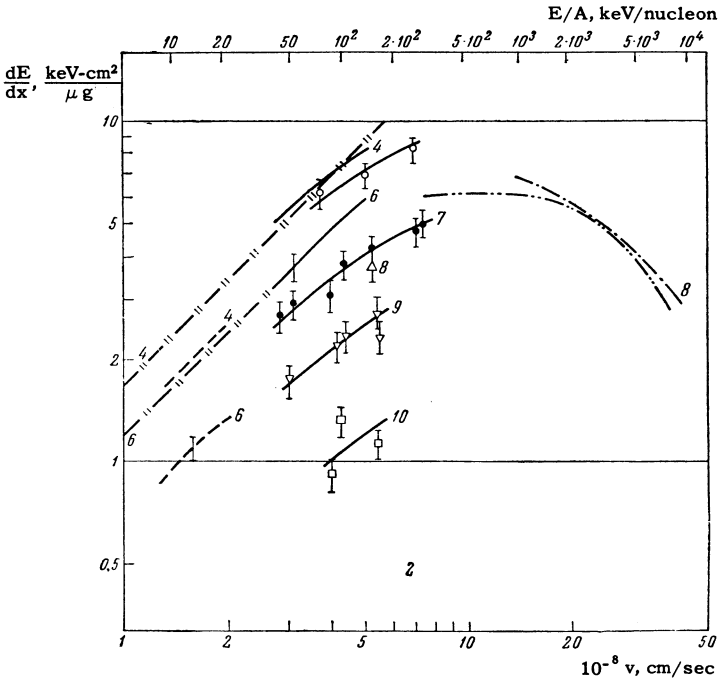

FIG. 4d

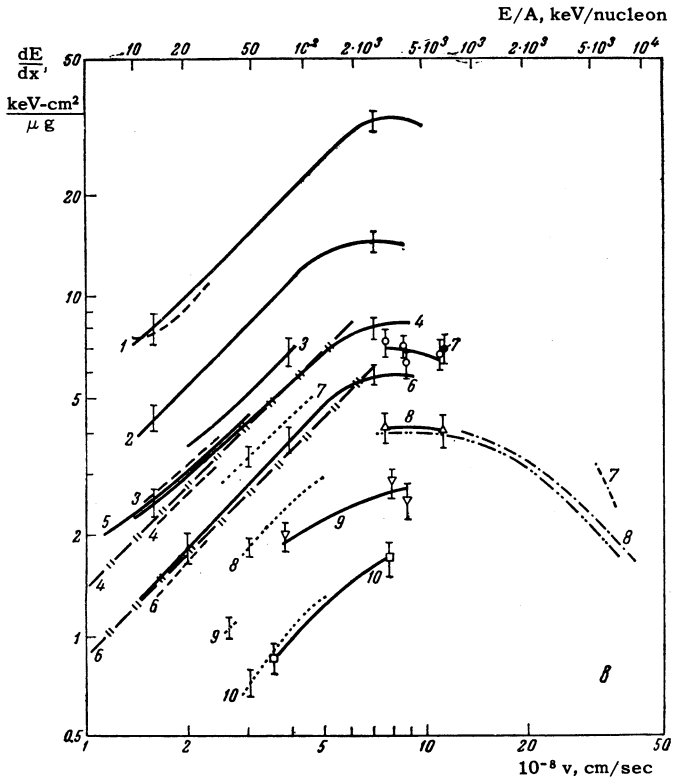

Fig. 4c

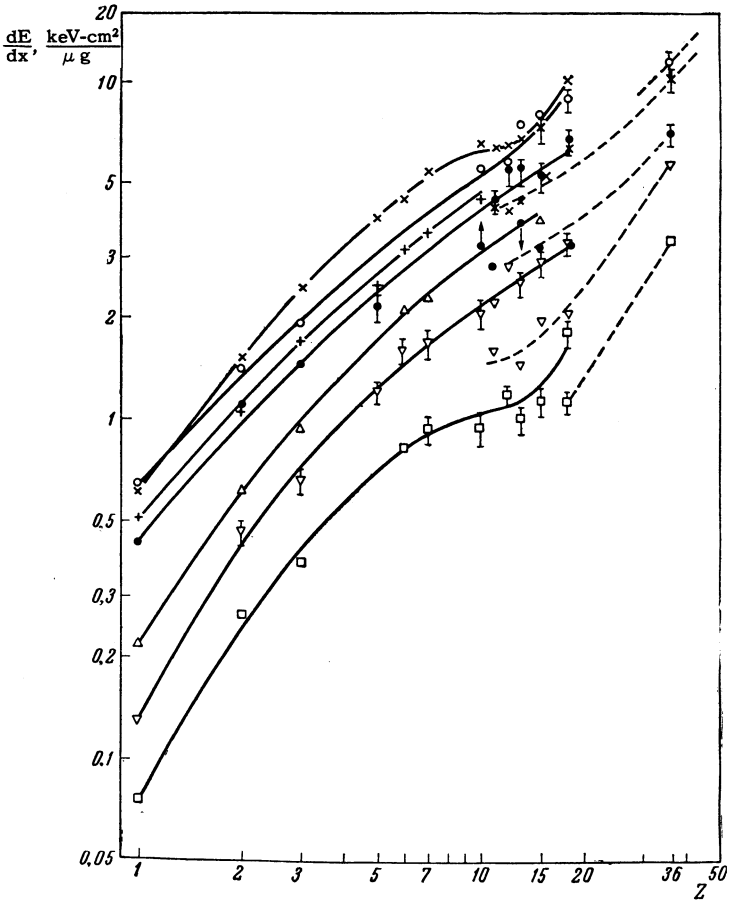

FIG. 5. Dependence of dE/dx on Z. × in air, + in argon, o in celluloid, • in Al, △ in Ni, ▽ in Ag, □ in Au. Continuous lines – $v = 3.7 \times 10^8$ cm/sec; dashed lines – $v = 2.35 \times 10^8$ cm/sec. The vertical bars represent maximum errors.

The curves representing dE/dx as a function of v agreed within ±5—10% with the values of dE/dx given in [7] for ions from He to Ne in hydrogen, air, and argon, and correspondingly with the data of other authors whose results were analyzed in [7].

For ions from Na to Kr, dE/dx was measured in air at velocities from 10^8 to 4×10^8 cm/sec (Fig. 5). In addition, the specific energy losses of ions from He to Kr were measured in celluloid, Al, Ni, Ag, and Au at several velocities (Figs. 4, 5, and 6). The measurements of dE/dx for He ions over the entire velocity range and for N ions from 2.5×10^8 to $\sim 5 \times 10^8$ cm/sec agreed within experimental error limits with the values obtained in [4] and [9].

It was pointed out in [7] that the curves of dE/dx as a function of v (Fig. 4) resemble the Bragg curve for α particles. These curves can be represented qualitatively by $dE/dx \approx v^m f(Z_S, Z)$ where m is close to unity at velocities up to $\sim 8 \times 10^8$ cm/sec, diminishes to zero at higher velocities, and is negative, approaching −2, for $v \geq 12 \times 10^8$ cm/sec.

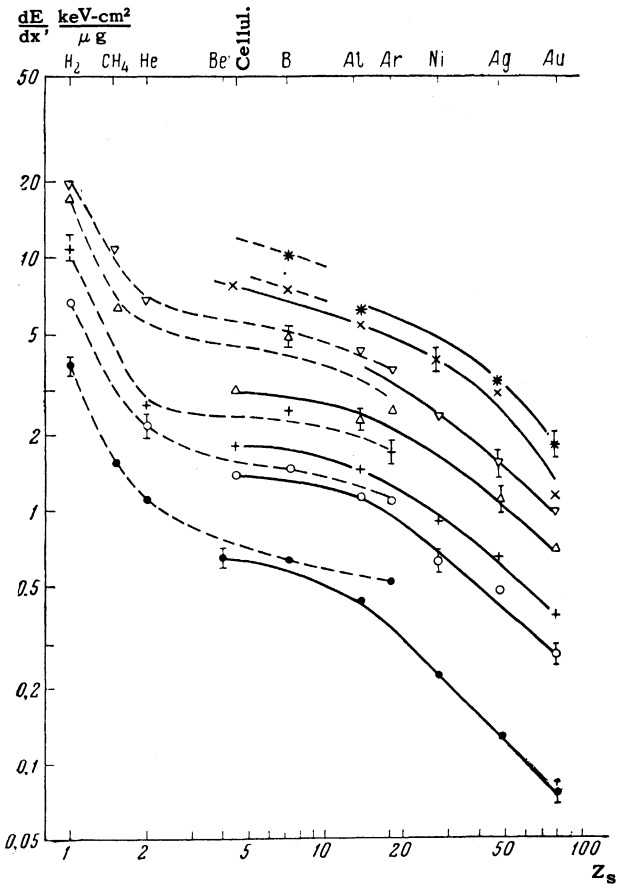

FIG. 6. Dependence of dE/dx on Z_S for ions: • – protons, o – He, + – Li, △ – B, ▽ – N, × – P, * – Ar; $v = 3.7 \times 10^8$ cm/sec. Continuous lines – in solids; dashed lines – in gases.

The position of the maximum of a dE/dx curve depends strongly on Z and to a lesser extent on Z_S. (In analyzing these relations we used the data of other authors for multicharged ions,[1-5,19] and relatively more precise measurements for protons and α particles.[9]) With increasing Z or Z_S the maximum is displaced toward higher velocities. As Z increases from 1 to 36 the maximum shifts from 3.5×10^8 to 14×10^8 cm/sec. As Z_S increases from 1 to 79 there is a shift of $\sim 2 \times 10^8$ cm/sec for light ions and even less for heavy ions.

The dependence of $(dE/dx)_{max}$ on Z is similar in all stopping media for $Z \geq 4$, with a slope of 1 ± 0.2 for $\log (dE/dx)_{max}$ versus log Z. For light ions ($Z < 4$) the slope of $\log (dE/dx)_{max}$ increases from 1.2 to 2.1 as Z_S increases from 1 to 79. An identical slope for light and heavy ions occurs only in the case of hydrogen. Therefore the dependence of $(dE/dx)_{max}$ on Z and Z_S for each ion group can be represented analytically by

$$(dE/dx)_{max} \sim Z^{f(Z_S)}.$$

The absolute values of dE/dx increase proportionally to Z on the average (Fig. 5). For ions from C to Al the rate of increase is slower, but reverts to the previous rate for still higher Z. The dependence of dE/dx on Z agrees qualitatively with the dependence of $\bar{i}^2$ on Z.[10] With increasing Z_S, dE/dx (in keV-cm²/μg) diminishes. The experimental points are grouped along two different curves (Fig. 6) for gaseous and solid media. However, approximately similar dependences dE/dx on Z_S are found for all ions including protons.

The ratio of dE/dx in two different media depends on the ion velocity; this dependence becomes stronger with an increased difference in Z_S. The ratio between dE/dx in hydrogen and other media is approximately proportional to $\sim v^{-\kappa}$, where $\kappa \sim Z_S^{0.6}$. The ratio of dE/dx in two different solids is more nearly constant, and is inversely proportional to density.

Beginning with $v > 5 \times 10^8$ cm/sec the ratio of dE/dx for multicharged ions in any two media agrees within ±15—20% with the results for protons. This agreement is not exact because dE/dx depends differently on Z_S for protons and multicharged ions. For protons $dE/dx \sim Z_S g(v, Z)$ on the average, while for multicharged ions $dE/dx \sim Z_S^{2/3} g(v, Z)$ in both solids and gases.[7]

The dependence of the quantity $B' = (dE/dx)/\bar{i}^2$, which is proportional to the stopping power, on Z

and Z_S varies with the ion velocity. At $v > (7-8) \times 10^8$ cm/sec B′ for all ions in any medium can be represented within experimental error limits by a single function B′(v). This is a power of v resembling that for protons: $B'(v) \sim v^{-n}$, where $n \approx f(Z_S)$, and changes from 0.85 to 1.85 as Z_S increases from 1 to 79. At $v < (7-8) \times 10^8$ cm/sec, B′ varies with Z, although the previous slopes of the B′(v) curves are retained on the average. The maximum of B′ is reached for Z equal to 2 or 3. With increasing Z, the value of B′ then decreases, but more rapidly in solids than in gases (Fig. 7).

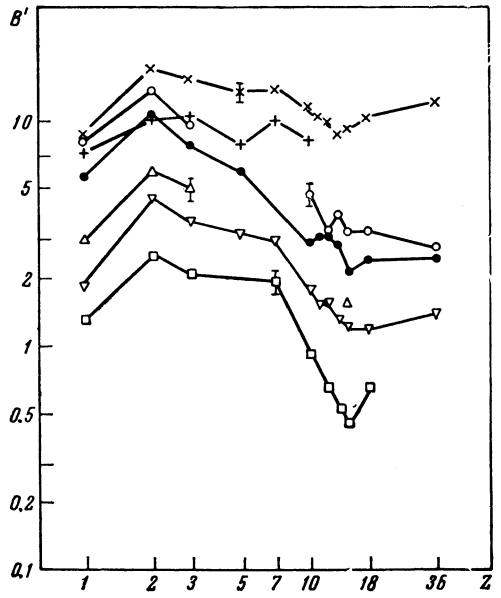

FIG. 7. Dependence of $B' = (dE/dx)/\overline{i^2}$ on Z: × in air, o in celluloid, + in argon, ● in Al, △ in Ni, ▽ in Ag, □ in Au. $v = 3.7 \times 10^8$ cm/sec.

In the formula $B' \approx Av^{-n}$ both A and n depend on Z and Z_S; these dependences are stronger for A. For $v < 7 \times 10^8$ cm/sec, $A \sim Z^{-\beta}$, where β approaches the value 2. As Z_S increases from 1 to 79, A decreases by 1.5—2 orders of magnitude. In the same range of Z_S (1—79) the value of n decreases by a factor of only ~ 1.5.

2. Discussion of results. A charged particle is slowed down in matter as a result of three basic processes: a) inelastic collisions between ions and atomic electrons of the medium, inducing the ionization and excitation of atoms, b) elastic collisions with atoms, and c) charge exchange at low velocities:[20,21]

$$-dE/dx = (dE/dx)_e + (dE/dx)_n + (dE/dx)_{ch}.$$

While the last two processes can be neglected for the larger part of the range of a singly-charged particle, and the first process can be partially neglected for fission fragments, multicharged ions represent an intermediate case when all three processes must be taken into account. The specific difference between multicharged ions and protons lies, first, in the fact that the charge-instability region extends to higher velocities. Second, because of the greater extent of the ionic field (as compared with a point charge), in close collisions an electron can pass through an ion, inducing a strong perturbation, while in distant collisions an ion can tear an electron away from a neutral atom even outside of the adiabatic limit v/ω_i (i.e., the impact parameter exceeds v/ω_i), where ω_i is the intrinsic frequency of electronic oscillations in the atom.[17]

The relative magnitudes of the roles played by the foregoing three processes depend on the ion velocity. The velocity interval considered in the present work lies within the theoretical limits between which calculations are possible. Therefore the experimental data can be used to compute the contributions of the different processes. In computing the energy loss due to inelastic collisions we used Bohr's classical formula for interaction in a screened field.[4,16] For nitrogen ions $(dE/dx)_n$ comprises less than 1% of the experimental value of dE/dx. However, for Ne ions at $v = (2.5-5) \times 10^8$ cm/sec this loss increases to 2—7%, and for P and Ar ions to 6—15%, depending on the stopping medium, and for Kr ions reaches 25—30% (Table III). The magnitude of $(dE/dx)_n$ diminishes at still higher velocities.

The value of $(dE/dx)_{ch}$ was computed from the formula

$$-(dE/dx)_{ch} = N\Sigma\Phi_i\sigma_{i,i-1}(J + E_k),$$

where N is the number of atoms per cm^3 of the stopping material, Φ_i is the fraction of ions with charge i in the equilibrium distribution, $\sigma_{i,i-1}$ is the cross section for electron capture by an ion with charge i,[10,20,21] J is the binding energy of electrons in molecules of the medium, $E_k = \mu v^2/2$ is the kinetic energy of an electron that was captured and subsequently lost by an ion, and μ is the electron mass. The function $(dE/dx)_{ch}(v)$ has a maximum at $v \sim (2-4) \times 10^8$ cm/sec, which is displaced somewhat toward higher velocities as Z_S increases. A relatively large fraction of the energy is lost through charge exchange when $v < v_0$. For He and Li ions this amounts to 25% of the total energy loss in helium, 7% in air, and 10% in argon. As Z increases, $(dE/dx)_{ch}$ is enhanced, although its ratio to the total energy loss remains approximately constant. For $v > v_0$ the contribu-

Table III

Ion	Stopping material	10^{-8} v, cm/sec	$\frac{dE}{dx}$, $\frac{keV\text{-}cm^2}{\mu g}$	$\left(\frac{dE}{dx}\right)_n$, $\frac{keV\text{-}cm^2}{\mu g}$	$\frac{dE}{dx}-\left(\frac{dE}{dx}\right)_n$	$\left(\frac{dE}{dx}\right)$ Firsov $\frac{keV\text{-}cm^2}{\mu g}$	$\left(\frac{dE}{dx}\right)_{ch}$, $\frac{keV\text{-}cm^2}{\mu g}$
N	Air	1.58	2.5	0.3	2.2	2.2	—
		2.19	3.2	0.2	3.0	3.0	—
		3.98	5.6	0.07	5.5	5.5	0.28
	Argon	1.58	1.4	0.2	1.2	1.4	—
		3.98	4.0	0.06	3.9	3.5	0.40
	Al	3.98	4.5	0.06	4.4	4.2	—
Ar	Air	3.98	10.6	0.43	10.2	9.8	0.38
	Al	3.98	7.1	0.37	6.7	6.4	—
	Ag	3.98	3.9	0.23	3.7	3.4	—
Kr	Au	2.45	3.5	1.3	2.2	2.0	—

Table IV

10^{-8} v, cm/sec	10^{15} dE/dx, eV-cm²/atom			
	N in argon	Ar in air	N in helium	He in air
2.6	170±17	170±20	30.5±3.0	29.2±1.5
3.2	195±15	210±20	36.6±3.0	34.3±1.7
4	250±20	250±20	46.1±4.0	38.1±1.9

tion of $(dE/dx)_{ch}$ drops sharply. Unlike the case of multicharged ions, for protons at $v \sim 1.5 \times 10^8$ cm/sec $(dE/dx)_{ch} = N\Sigma\Phi_i\sigma_{i,i-1}J$ is large. According to Allison, [21] it amounts to 43% in helium and 17% in hydrogen or air.

In the velocity region of multicharged ions that is of interest in the present work the "electronic" loss $(dE/dx)_e$ comprises 75—90% of the total energy loss.

To compute $(dE/dx)_e$ for protons in highly dense media (metals) up to 20 keV, when the specific loss is proportional to the particle velocity, we used the Fermi-Teller formula based on the calculation of the stopping of a singly-charged particle in a degenerate electron gas. [22,13] The experimental values of dE/dx given in [23] for protons in Ag exceed the theoretical computed values by ~ 50%. For multicharged ions the values of $(dE/dx)_e$ calculated from this formula and then multiplied by $\bar{i}^2$ [10] are 20—30% below the experimental values; for N ions in Ag at $v = v_0$ the discrepancy is 30%.

The specific energy losses $(dE/dx)_e$ in gases were computed using the energy ϵ transferred in an interaction between two atoms. Firsov [14] has calculated ϵ for electron motion in a self-consistent atomic field determined from the Thomas-Fermi model. In this calculation we have

$$dE/dx = \int_0^\infty \varepsilon 2\pi R_0\, dR_0,$$

where R_0 is the impact parameter. The formula

$$-dE/dx = 2.34\,(Z + Z_s)\,v \cdot 10^{-15}\ \text{eV}\cdot\text{cm}^2/\text{atom},$$

where v is in units of 10^8 cm/sec, was obtained by integration and is valid, as already indicated, for $Z_s \approx (\frac{1}{4}-4)Z$. This theory is compared with experiment in Table III. Firsov's formula for dE/dx agrees with experiment in the range where dE/dx is proportional to ion velocity. It should be noted that Firsov considers a multiple transfer of electrons from slowly moving systems, where the ion and atom are fully equivalent. The correctness of this treatment is confirmed by the equality of the experimental values of dE/dx for ion-atom "pair inversions" at low velocities. A comparison of dE/dx for N ions in argon and Ar ions in air showed equal specific energy losses within experimental error limits at v = const. The agreement is especially good at low velocities up to $v = 4 \times 10^8$ cm/sec. The difference increases with high velocities since the systems become non-equivalent as the initial ion charge is increased (Table IV).

At velocities $v > v_0$, i.e., in the region containing the maximum of dE/dx as a function of v, the ion charge $\bar{i}$ approaches Z. For example, we have the maximum degree of ionization $(\bar{i}/Z)_{max} \approx 0.8$ for He ions, and a value close to 0.6 for Ne ions. Therefore the shift of the maximum of dE/dx with increasing Z can be accounted for by the fact that Z is reached at a higher velocity of heavy ions than of light ions. Moreover, electrons begin to participate in the slowing-down of ions sooner in light media than in those with large Z_s; this shifts the maximum with increasing Z_s. Thus with increasing velocity $(v > v_0)$ the characteristics of

the electronic structure of ions begin to be effective. Therefore the Hartree-Fock method [24] should be used to compute electron density and ionization potentials instead of the Thomas-Fermi atomic model.

At velocities $v \gg u$, where u is the velocity of orbital electrons in atoms of the stopping material, $(dE/dx)_e$ can be computed using the quantum-mechanical formulas of Bethe and Bloch and the classical formula of Bohr. [8,16] In our velocity region these formulas were used to compute $(dE/dx)_e$ in a somewhat modified form, with account of charge exchange. Bloch's formula, which is more nearly universal than the other two formulas, was used in the form

$$-\left(\frac{dE}{dx}\right)_e = 9{,}56\cdot 10^{-15} Z_s^2 \frac{\overline{i^2}}{x^2}\left[0.848 + \ln\frac{x^3}{Z_s} - \Delta^*\right] \text{eV-cm}^2/\text{atom}$$

where

$$x = \frac{v}{v_0}, \qquad \Delta^* = \frac{\sum \Phi_i i^2 (\ln i + \Delta)}{\sum \Phi_i i^2},$$

$$\Delta = \left[\operatorname{Re}\psi\left(1 + j\frac{i}{x}\right) + \ln\frac{x}{i}\right], \qquad j = \sqrt{-1},$$

and the values of Φ_i and $\overline{i^2}$ were determined experimentally. [10] The value of $(dE/dx)_e$ computed from this formula for protons in hydrogen is only 5—7% lower than the measured value at $v \sim 4 \times 10^8$ cm/sec. For multicharged ions similar agreement is observed at large v. An example is given in Fig. 4b for B ions at $v \sim 11 \times 10^8$ cm/sec etc. (The curve labeled **B1** was not extended because of the lack of data for $\overline{i^2}$ and dE/dx.) With increasing Z_S and decreasing v there is growing divergence between theory and experiment.

When dE/dx is computed in materials with $Z_S > 1$ the condition $v \gg u$ is violated for inner-shell electrons of these media, thus decreasing their participation in the stopping process. This circumstance is expressed analytically by the fact that the mean ionization potential J in the logarithmic term

$$L = \frac{dE}{dx} \Big/ \frac{4\pi e^4 \overline{i^2} Z_S}{\mu v^2} = \ln\frac{2\mu v^2}{J},$$

of dE/dx ceases to remain constant and becomes a function of v. Lindhard and Scharff [17] used a semiempirical relation between L and v that agreed with Madsen's [12] experimental data within ±10%.

For all multicharged ions in gases and for Li, B, D, and N ions in solids the value of L(x) computed from experimental results for $\overline{i^2}$ and dE/dx was ~ 20% greater, while for ions from Na to Kr it was ~ 50% smaller, than for protons. These differences are not evidence of an increase or decrease, respectively, in the stopping power, but rather of a discrepancy between the square of the effective charge i^{*2} and $\overline{i^2}$.

In order to test this hypothesis the formula $dE/dx = i^{*2}(dE/dx)_p$ was used to compute the effective ion charge. This relation can be used if $B'(v, Z)$ is identical for all ions, as is true in first approximation, and i^{*2} is close to unity for protons. For $v \leq 4 \times 10^8$ cm/sec the effective proton charge is less than unity, but when the energy loss of the neutral component is taken into account the effective charge increases and approaches unity.

A comparison shows that for some light ions (He to Ne) at $v < 4 \times 10^8$ cm/sec i^{*2} exceeds $\overline{i^2}$ [10] by 10—20% (Fig. 8). With increasing velocity this discrepancy diminishes. [3] There is an approximately identical degree of difference between i^{*2} and $\overline{i^2}$ in solids and gases, but their absolute values are higher in solids; this has been noted at high velocities. [25] The general dependence of i^{*2} on Z_S in gases is similar to $\overline{i^2}(Z_S)$.

With increasing Z, i^{*2} becomes smaller than $\overline{i^2}$ in solids (Fig. 8), thus reversing the relationship. In gases we still have $i^{*2} > \overline{i^2}$, as for light ions.

The increase of i^{*2} compared with $\overline{i^2}$ indicates that a considerable fraction of the energy loss occurs in close collisions of an ion with electrons, when a charge greater than $\bar{i}$ can act upon an electron. In contrast, the difference between i^{*2} and $\overline{i^2}$ in solids is not associated with an actual

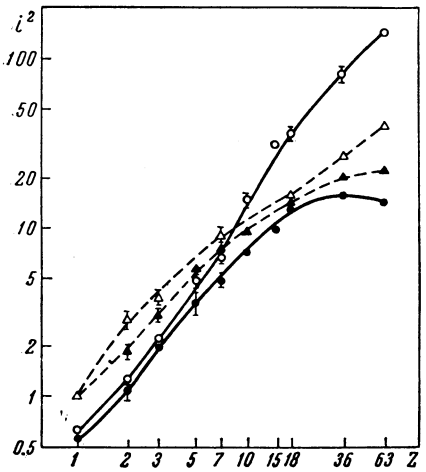

FIG. 8. Dependence of $\overline{i^2}$ (continuous lines) and of $\overline{i^{*2}}$ (dashed lines) on Z at $v = 3.16 \times 10^8$ cm/sec. o and • denote $\overline{i^2}$ in solids and gases, respectively; △ and ▲ denote i^{*2} in solids and gases, respectively. The data for fission fragments ($Z \sim 63$) were taken from [11] and [26].

decrease of ion charge, but with the fact that $B'(Z,v)$ depends on $\bar{i}$, decreasing as $\bar{i}$ increases. This dependence is represented qualitatively by Bloch's formula [7]

$$-dE/dx = B_0 - Z_{\text{eff}}\, Q\,(v/v_{0\bar{i}}),$$

where B_0 is constant and Q increases as $v/v_{0\bar{i}}$ decreases. The value of Z_{eff} is obtained experimentally. [7] We must note, in conclusion, that there is actually less difference between the behavior of $B'(Z)$ and $\overline{i^2}(Z)$ in solids and gases than would appear from Figs. 7 and 8, because our value of $\overline{i^2}$ pertains to a gas pressure $\sim 10^{-2}$ mm Hg, [10] while dE/dx was measured at pressures $\gtrsim 40$ mm Hg.

We are deeply indebted to S. S. Vasil'ev for his interest, to the cyclotron crew, especially A. A. Danilov, M. Kh. Listov, and V. P. Khlapov, and to O. B. Firsov for a valuable discussion of the relationship between the experimental results and the theory.

[1] Heckman, Perkins, Simon, Smith, and Barkas, Phys. Rev. **117**, 544 (1960).

[2] P. G. Roll and F. E. Steigert, Nuclear Phys. **17**, 54 (1960).

[3] L. C. Northcliffe, Phys. Rev. Letters **5**, 353 (1960); Phys. Rev. **120**, 1744 (1960); Schambra, Rauth, and Northcliffe, Phys. Rev. **120**, 1758 (1960).

[4] D. I. Porat and K. Ramavataram, Nuclear Instr. and Methods **4**, 239 (1959); Proc. Roy. Soc. (London) **A252**, 394 (1959).

[5] D. I. Porat and K. Ramavataram, Proc. Phys. Soc. (London) **77**, 97 (1961).

[6] Teplova, Nikolaev, Dmitriev, and Fateeva, Izv. AN SSSR Ser. Fiz. **23**, 894 (1959), Columbia Tech. transl. p. 883.

[7] Teplova, Nikolaev, Dmitriev, and Fateeva, JETP **34**, 559 (1958), Soviet Phys. JETP **7**, 387 (1958).

[8] H. A. Bethe and J. Ashkin, in Experimental Nuclear Physics, edited by E. Sergè (John Wiley and Sons, New York, 1953), Vol. 1, p. 166.

[9] W. Whaling, in Handbuch der Physik, edited by S. Flügge (Springer-Verlag, Berlin, 1958), Vol. **34**, p. 193.

[10] Nikolaev, Dmitriev, Fateeva, and Teplova, JETP **39**, 905 (1960) and **40**, 989 (1961); Soviet Phys. JETP **12**, 627 (1961) and **13**, 695 (1961).

[11] J. M. Alexander and M. F. Gazdik, Phys. Rev. **120**, 874 (1960).

[12] C. B. Madsen, Kgl. Danske Videnskab. Selskab, Mat.-fys. Medd **27**, No. 13, 1953.

[13] E. Fermi and E. Teller, Phys. Rev. **72**, 399 (1947).

[14] O. B. Firsov, JETP **36**, 1517 (1959), Soviet Phys. JETP **9**, 1076 (1959).

[15] L. Winsberg and J. M. Alexander, Phys. Rev. **121**, 518 (1961).

[16] N. Bohr, The Penetration of Atomic Particles Through Matter, Kgl. Danske Videnskab. Selskab, Mat.-fys. Medd. **18**, No. 8 (1948).

[17] J. Lindhard and M. Scharff, Kgl. Danske Videnskab. Selskab, Mat.-fys. Medd. **27**, No. 15 (1953); J. Lindhard, in Niels Bohr and the Development of Physics, edited by W. Pauli (McGraw-Hill, New York, 1955), p. 244.

[18] R. M. Sternheimer, Phys. Rev. **117**, 485 (1960).

[19] Yu. Ts. Oganesyan, JETP **36**, 936 (1959), Soviet Phys. JETP **9**, 661 (1959).

[20] S. K. Allison and S. D. Warshaw, Revs. Modern Phys. **25**, 779 (1953).

[21] S. K. Allison, Revs. Modern Phys. **30**, 1137 (1958); Allison, Cuevas, and Garcia-Munoz, Phys. Rev. **120**, 1266 (1960).

[22] S. D. Warshaw, Phys. Rev. **76**, 1759 (1949).

[23] V. G. Tel'kovskii and V. I. Pistunovich, DAN SSSR **113**, 1035 (1957), Soviet Phys.-Doklady **2**, 184 (1958).

[24] M. Gryzinski, Phys. Rev. **107**, 1471 (1957).

[25] P. G. Roll and F. E. Steigert, Phys. Rev. **120**, 470 (1960).

[26] N. O. Lassen, Kgl. Danske Videnskab. Selskab, Mat.-fys. Medd. **25**, No. 11, (1949).

Translated by I. Emin
7